Al-Azhar University Civil Engineering Research Magazine (CERM)
Vol. (44) No. (3) october . 2022

BEHAVIOR OF REINFORCED CONCRETE SHEAR WALLS UNDER BLAST LOADING

Ahmed T. Nasr[1], Tarek El-Hashimy[2], Khaled M. Abdelgawad[3], M. N. Fayed[4]

[1](Structural Engineer, Post-Graduate Student, Faculty of Engineering, Ain Shams University, Egypt)
[2](Assistant Professor, Structural Engineering Department, Faculty of Engineering, Ain Shams University, Egypt)
[3](Lecturer of Civil Defense, Police Academy, Egypt)
[4](Professor of Structural Analysis, Structural Engineering Department, Faculty of Engineering, Ain Shams University, Egypt)

الملخص العربى:

نتيجة للحوادث الإرهابية المتكررة في جميع أنحاء العالم التي تستهدف منشآت البنية التحتية والمنشآت البارزة، حظيت دراسة المنشآت تحت تأثير الأحمال الناتجة عن الموجات الانفجارية (أحمال الانفجار) باهتمام كبير في السنوات الأخيرة. الهدف من هذه الدراسة هو التحقق من سلوك الأنظمة الإنشائية المختلفة لحوائط القص الخرسانية المسلحة تحت احمال الانفجار. تمت محاكاة نموذج العناصر المحددة وتم التحقق من صحته بالنتائج التجريبية في الابحاث وأظهر نتائج فعالة ودقيقة لسلوك البلاطات الخرسانية المسلحة تحت حمل الانفجار. في هذا البحث، تم محاكاة ثلاثة مبانٍ خرسانية مسلحة مكونة من 8 طوابق بتكوينات مختلفة تحت موجة انفجار بوزن شحنة يبلغ 1000 كجم من مادة تي إن تي ومسافة تبلغ 15 مترًا باستخدام النماذج ثلاثية الأبعاد. تم تمثيل حمل الانفجار على كل عنصر انشائي (الحوائط، الكمرات و الأعمدة) على الواجهة الأمامية للمبنى في نموذج ثلاثي الأبعاد. وتم عمل تحليل ديناميكي غير خطي لتحديد قيمه الحمل على أساس المساحه التي يدعمها العنصرالانشائي، ومسافة المواجهة الفعلية بين موقع الشحنة و مركز العنصر، وزاوية السقوط بين مركز الموجة و مركز كل عنصر. تبحث الدراسة في الاستجابة الكلية للمنشئات الخرسانية المسلحة بالإضافة إلى استجابة العناصر الجزئية تحت تاثير حمل الانفجار.

الكلمات الدالة : أحمال الانفجار – خرسانة مسلحة – العناصر المحددة – الاستجابة الكلية – الاستجابة الجزئية.

ABSTRACT:

As a result of repeated terrorist incidents around the world that target important structures, blast loads have received great interest in recent years. The goal of this study is to investigate behavior of different reinforced concrete shear-wall structural systems under blast loading. A finite element model is simulated using SAP2000 v23 and validated with experimental results in literature and showed efficient and accurate results for the behavior of reinforced concrete panels under blast loading. In this research, three reinforced concrete 8-story buildings with different configurations under blast wave of explosive weight of 1000 Kg TNT and standoff distance of 15m are simulated with 3D finite element models. Their analyses are done by applying blast load at each structural element (wall, beam and column) on front face of the building. The load time-history is determined based on the tributary area supported by the element, the actual stand-off distance between the charge location and the joint under consideration (center of structural element), and the

angle of incidence between the wave front and the center of each element. The study investigates the global response of reinforced concrete structures in addition to the response of their individual members under blast loading conditions.

KEYWORDS: Blast Load; Reinforced Concrete; Finite Element; Global Response; Local Response.

1- INTRODUCTION

Reinforced concrete shear walls are designed to resist not only gravity loads and in-plane seismic force but out-of-plane loads as well. Although shear wall failure due to out-of-plane loading can lead to progressive collapse of buildings, there have been fewer investigations on out-of-plane performance and failure of shear walls than on in-plane performance. Some researchers compared the performance of buildings under seismic in-plane loading and blast out-of-plane loading. Others compared the performance of various structural systems under blast loads.

The performance of buildings under blast loading has to be considered for blast-resistant buildings as well as their performance under seismic loading. Dan Nourzadeh et al. [1] compared between the global response of reinforced concrete building under seismic loading and blast loading. In this study, a 10-story reinforced concrete building is simulated in Opensees software using nonlinear beam-column elements. The building is exposed to ten distinct seismic ground movements reflecting two different hazard levels (eastern and western regions of Canada), as well as two moderate far-field blast load levels at 15 m and 30 m standoff distances with explosive weights of 1000 Kg. The inter-story drifts induced in the building as a result of the blast loading were found to be much greater than those caused by design- and higher-than-design-basis earthquakes. As a result, it is concluded that the blast loads may cause the structure to deform laterally with magnitudes comparable to or greater than those encountered under seismic loads.

Studying the response of different concrete materials under blast loading, Wu et al. [2] tested reinforced concrete slabs with regular reinforced concrete (NRC), reinforced concrete reinforced with FRP plates, unreinforced ultra-high-performance concrete (UHPFC), and reinforced ultra-high-performance concrete (RUHPFC) under blast loading. A series of explosion tests on slabs helped to attain the goal of this study. To analyze the pressure distribution on the slabs, air blast pressure histories were recorded at the center and edge of the slabs. The overpressure measured at the mid-point of the slab was much greater than the overpressure recorded at the lower point of the slab, indicating that the blast pressure on the slab was not uniform, which was an expected outcome given the short standoff distance. This demonstrates that the angle of incident between the explosion source and the structural element must be addressed and not ignored. It is also concluded that when exposed to comparable blast loads, the plain UHPFC slab experienced less damage than the NRC slabs.

Focusing on the behavior of reinforced concrete structures under blast loading, however the global response of the building structures can be important in blast loading, 2D model was quite adequate for determining the response of a regular building and the

2D model also reduced the computational efforts significantly (Dan Nourzadeh et al. [3] and Naito et al. [4]). While other researchers studied only the global response of reinforced concrete buildings under blast loading (Shallan et al. [5]). Under blast loading, Shallan et al. [5] did numerical models for three reinforced concrete two-story structures with varied aspect ratios. It is concluded that the reflected overpressure of blast load decreases with increasing the standoff distance from the building while the arrival time increases. Furthermore, although there is no variation in the displacement of the column in the face of the blast load with variation in the aspect ratios of the buildings, the effect of blast load decreases in other elements in the building far from the detonation point with increasing the aspect ratio of the buildings. On the other hand, Naito et al. [4] investigated the global and local responses of a reinforced concrete shear wall building subjected to blast loading. This building was three stories high with shear walls at the corners and was designed for a high seismic zone. It is concluded that for stiff walls, the dynamic analysis can be simplified by establishing a "component" model with fixed-fixed end conditions. The component model overestimates resistance at the collapse stage for an impulsive blast demand by 7%. While this is a minor change, it should be kept in mind that the component model results will always be unconservative since the wall is assumed to be stiffer than actuality. Also, Dan Nourzadeh et al. [3] analyzed 2D and 3D models for two 10-story reinforced concrete buildings subjected to a series of blast loads. The progressive collapse of different lateral load resisting systems was examined by Chehab et al. [6]. In this research, five structures designed as moment-resisting frames and nine designed as shear wall systems with different number of stories and number of bays. In addition, many researches handled the progressive collapse of buildings under the effect of blast load as Izzuddin et al. [7], McConnell et al. [8] and Shi et al. [9].

Taking into consideration different methods of analyses of buildings under blast loading, Naito et al. [4] analyzed reinforced concrete shear wall building under two stages. In the first stage, a nonlinear static pushover analysis was performed on the structural system using DIANA 3D finite element model to identify the location of failure. The pressure was assumed to act uniformly over each segment of the wall normal to the surface. The second stage involved creating a simplified single degree of freedom model on the vulnerable portion of the structure in order to simulate the inelastic dynamic response under blast loading. While Dan Nourzadeh et al. [3] studied different patterns of applying blast load in finite element analysis. The difference between the patterns is how the blast pressure is calculated at different joints, then this pressure is added based on the tributary area of each joint. Among the various blast load patterns tested, it was determined that loading all components at a story with the shortest standoff distance and the greatest incident angle to the story results in a response that is closest to that obtained from the exact progressive pattern of load application. To save time and effort, the variations in blast loads on different nodes in a story based on their distance to charge and incident angles to the blast wave might be ignored. On the other hand, simultaneous loading of the entire building using the shortest standoff distance results in excessive and unrealistic estimates of structural deformations.

In addition, Draganic et al. [10] used SAP2000 to establish that it is feasible to model an explosive effect and provide a preliminary assessment of the structure using conventional software. Three close blast waves with varying explosive charges (1 kg, 10 kg, and 100 kg) were simulated on a multi-story reinforced concrete mixed frame-wall building. This study concludes that non-linear analysis is required and that simple plastic hinge behaviour is adequate. Also, the post analysis is important to check the redistribution of loads after the failure of some structural elements as well as checking the progressive collapse. It is also concluded that in elements exposed to distant explosions, conventional reinforcement provides sufficient ductility, while for close explosions additional reinforcement is needed. While Meena et al. [11] studied three buildings had different patterns of walls using nonlinear finite element model with ETABS software.

The goal of this study is to investigate the local and global behavior of different reinforced concrete shear-wall structural systems under blast loading. This is done by simulating three different systems for 8-story reinforced concrete building under blast wave of explosive weight of 1000 Kg and standoff distance of 15m. The buildings are simulated with finite element modelling using SAP2000 v23 software for simulating the 3D model of the building, the multi-layered reinforced concrete walls and the dynamic blast loading.

2- BLAST LOADS ESTIMATION

A blast wave, as illustrated by Figure (1), is distinguished by an immediate increase in pressure above ambient air pressure in a brief period of time, followed by pressure decline as the wave extends outward from the explosion source owing to energy dissipation. Furthermore, blast wave impulse (I) is one of the most essential blast wave categories. The blast wave impulse may be defined as the region contained by the pressure time curve.

$$I = \int P(t)\, dt \qquad (1)$$

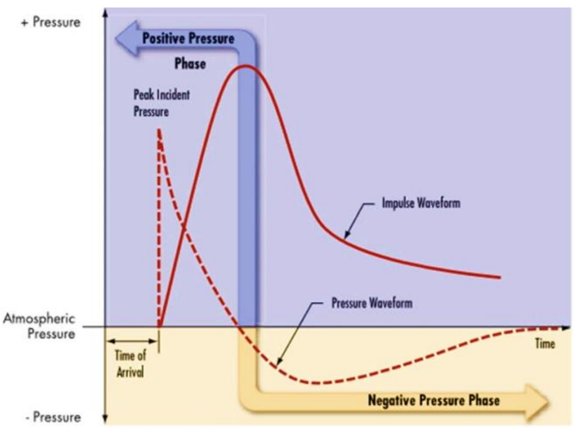

Figure 1: Typical Pressure-Time Curve (FEMA-356)

The pressure-time curve is typically divided into two phases: a positive phase where the incident/reflected pressure reduces to its ambient value, and a negative phase when the pressure drops below the ambient pressure. (td) indicates the positive phase duration of the actual blast wave, whereas (Po) represents the peak reflected pressure of the blast wave. Due to its low pressure (i.e., absolute magnitude) and long duration in comparison to the positive phase, the negative phase is typically not considered in blast design (Krauthammer [12]). Scaled distance (Z) of a blast wave is determined by the explosive material's equivalent charge weight (W) and the standoff distance from the detonation source (R).

$$Z = R/W \wedge (1/3) \quad (2)$$

According to UFC 3-340-02 [13], blast loads are classified into two types based on the confinement of an explosive charge which are confined and unconfined blast loads. This research focuses on unconfined explosions which are divided into three types, free air burst, air burst and surface burst.

2.1- Free Air Burst

Free-air blast pressures occurs when an explosive source bursts near or above a protective structure as shown in Figure (2), there is no amplification of the initial shock wave between the explosive source and the protective structure [14]. The incident wave will collide with the structure as it advances radially out from the explosion's source, reinforcing and reflecting the initial wave (pressure and impulse) as illustrated in Figure (3).

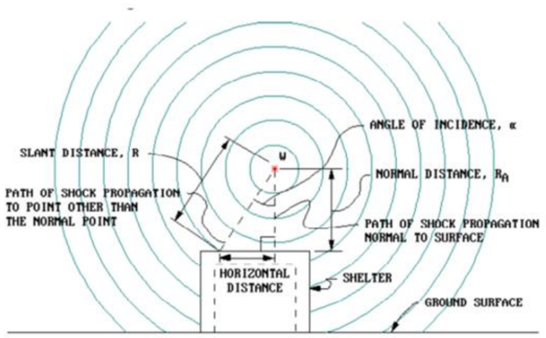

Figure 2: Free Air Burst (UFC 3-340-02 [13])

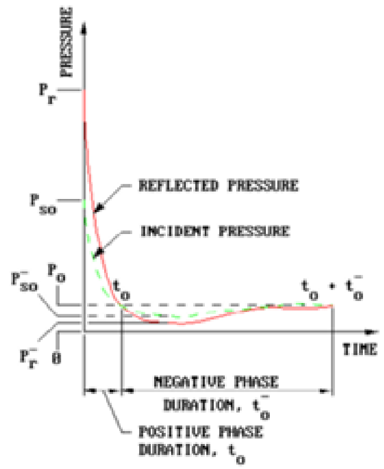

Figure 3: Pressure-Time Variation for a Free Air Burst (UFC 3-340-02 [13])

Figure (2-7) in UFC 3-340-02 [13] can be used to determine the positive phase pressures, impulses, durations, and other shock environment characteristics for spherical TNT explosions versus the scaled distance (Z). While the negative phase parameters are determined from Figure (2-8) in UFC 3-340-02 [13]. Free air burst is used in the model validation in this research.

2.2- Air Burst

The explosion in the air is a phenomenon caused by the detonation of explosives above ground level at a distance from the structure as shown in Figure (4), resulting in the ground's reflection of the blast wave. The ground's reflection amplifies the initial wave, producing the reflected wave. Although there are pressure variations over the front height, for the purposes of the analysis, they are ignored and regarded as a plane wave. The parameters are computed as for a ground explosion. Peak reflected pressure ($P_{r\alpha}$) is determined using Figure (2-9) in UFC 3-340-02 [13]، using the scaled charge height above the ground (Hc/W ^ 1/3) and the wave angle α. A similar procedure is applied to determine the impulse ($I_{r\alpha}$).

2.3- Surface Burst

The explosion is referred to be near the ground if the charge is placed very close to or on the ground. The reflected wave is formed when the initial blast wave is reflected and amplified by ground reflection. In contrast to an explosion in the air, the reflected wave merges with the initial wave at the detonation point, forming a single wave as illustrated in Figure (5), which will be used and discussed in depth in our study.

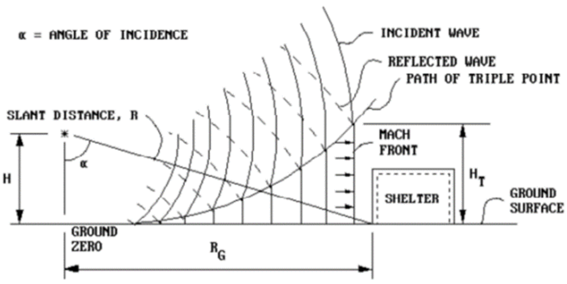

Figure 4: Air Burst (UFC 3-340-02 [13])

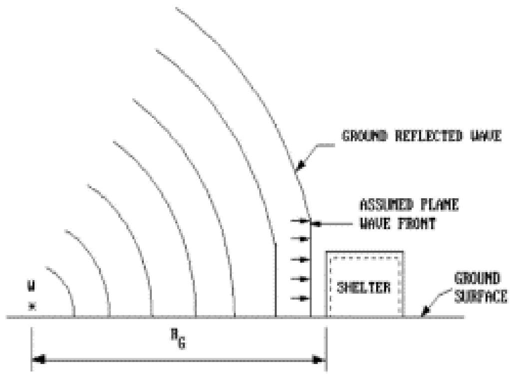

Figure 5: Surface Burst (UFC 3-340-02 [13])

3- FINITE ELEMENT MODELLING

In this study, the building configurations were modelled geometrically in the three dimensions using finite element modelling using SAP2000 v23 software to study the response of these buildings under the dynamic blast loading.

3.1- Material Model

Two types of concrete material are defined. The unconfined concrete model represents the concrete with no confinement for shear walls and slabs, confined concrete model represents the concrete for the beams and columns surrounded by ties with compressive strength calculated according to Mander et al. [15], based on the transverse reinforcement used to enhance the member strength and ductility. Material nonlinearity is incorporated into the finite element model (SAP 2000) by using Mander model for concrete (Takeda hysteresis type) and simple model for steel (Kinematic hysteresis type).

3.2- Model Geometry

Nonlinear layered shells for shear walls and slabs are modelled by a multi-layer shell element, which is based on the concrete model proposed by Miao et al., [16]. A multi-layer shell element model - based on composite material mechanics principles - was used to simulate the coupled in-plane/out-of-plane bending or coupled in-plane bending-shear nonlinear behaviors of the reinforced concrete shear wall. In multi-layer shell element model, the shell element is composed of several layers of varying thicknesses. Different layers are assigned different material properties. Unconfined concrete material is assigned to the middle layer, surrounded by a layer of vertical rebar and a layer of horizontal rebar from each side. In defining the geometry for the 3D model, the floors were assumed to act as semi rigid diaphragms.

In order to examine the plastic behavior of the structure, frame elements for beams and columns with plastic hinges according to ASCE 4-13 [17] are allocated at start and end relative distances of 0.05 and 0.95. Plastic hinge type assigned to columns is interacting (P-M2-M3). And assigned to beams is M3 type which is single moment rotation type as per ASCE 41-13 [17]. The nodes at the base of the building structure were restrained along all degrees of freedom representing fully fixed supports. While the boundary condition of the walls (Wu et al., [2]) used in model validation were fixed in translation and free in rotational (hinged supports).

3.3- Plastic Hinges Definition

FEMA-356 [18] defines the hinge rotation behavior of reinforced concrete members through the five points (A, B, C, D, and E) illustrated in Figure (6). The deformations are expressed as per the figure using terms like strain, curvature, rotation, or elongation. The parameters a and b shall refer to the plastic deformation that occurs after yield (after point B). The parameter c represents the reduced resistance after the sudden change from C to D. ASCE 41-13 [17] defines numerically the parameters a, b, and c. The points on the figure can be explained as the following:

- Point A is always the origin.
- Point B represents yielding. No deformation occurs in the hinge up to point B, regard less of the deformation value specified for point B. The displacement (rotation) at point B will be subtracted from the deformations at points C, D, and E. Only the plastic deformation beyond point B will be exhibited by the hinge.
- Point C represents the ultimate capacity for push over anal y sis. However, you may specify a positive slope from C to D for other purposes.
- Point D represents a residual strength for push over analysis. However, you may specify a positive slope from C to D or D to E for other purposes.
- Point E represents total failure. Beyond point E the hinge will drop load down to point F (not shown) directly be low point E on the horizontal axis.

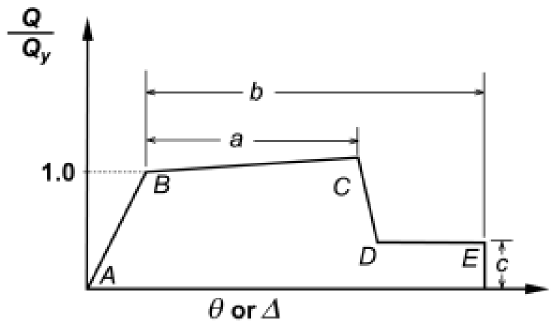

Figure 6: Generalized Force – Deformation Curve (FEMA – 356 [18])

3.4- Dynamic Blast Loading

The blast dynamic loading applied in the model as a time history analysis (transient analysis). The load applied as a multiplication of a load pattern and a function. Load pattern represents the tributary area for each element and assigned as a line load for beams and columns and area load for walls. While the function represents the Pressure-Time curve of blast waves applied on the structural components. The nonlinear dynamic analysis was performed by means of step-by-step integration using Hilber-Hughes-Taylor. The damping effects are also considered with constant damping ratio for all modes of 5% as suggested by CSA S850-12 [19]. Before analyzing the structure for the dynamic blast loads, an Eigen-value analysis was carried out to obtain the natural periods of the structure.

For the dynamic models, since blast loads are characterized by very high loading rates, Dynamic Increase Factors (DIFs) are applied to the material properties to account for high strain rate effects, Dynamic increase factors of 1.25 and 1.23 were applied to the compressive strength for concrete and yield strength steel reinforcing bars, respectively, according to UFC 3-340-02 [13].

4- FINITE ELEMENT MODEL VALIDATION

Three tested slabs from Wu et al. [2] were used in the finite element model validation. These slabs are 1000mm width X 1800mm height X 100 mm thickness. The three specimens (NRC-1, NRC-2 and NRC-3) were simply supported on two short edges and constructed with a 12 mm diameter mesh that was spaced at 100 mm centers in the major bending plane (ρ = 1.34%) and at 200 mm centers in the minor plane (ρ = 0.74%). The thickness of the concrete cover was 10 mm. The concrete had a cylinder compressive strength of 39.5 MPa, tensile strength of 8.2 MPa and Young's modulus of 28.3 GPa. The reinforcement had a yield strength of 600 MPa and Young's modulus of 200 GPa.

The slabs are subjected to incident overpressures produced by detonating cylindrical-shaped charges (Composition B) at different scaled distances (between 0.93 and 3.0 m/kg1/3) in free air. Specimen NRC-1 and NRC-2 were subjected to 1 and 8 kg of equivalent TNT explosives located 3.0 m away above the panels' central points. While specimen NRC-3 was subjected to 3.4 kg of equivalent TNT explosives located 1.4 m. During the validation of the dynamic model response, the blast wave (i.e., pressure–time response history) produced by these charges was used as a time-series load in SAP 2000 as per UFC 3-340-02 [12]. Wu et al. [2] used two pressure transducers to measure air blast pressures both at the center of the specimen (PT1) and near one support (PT2) as shown in Figure (7). According to Wu et al. [2], no cracking was observed in specimens NRC-1 and NRC-2 after testing while fine cracks of negligible residual width were observed in NRC-3 as shown in Figure (8), but it is unlikely that the yield moment in the slab was reached. In addition, Table (1) shows the blast waves parameters added in the finite element model on the three specimens based on UFC 3-340-02 [13], which confirms with the experimental results.

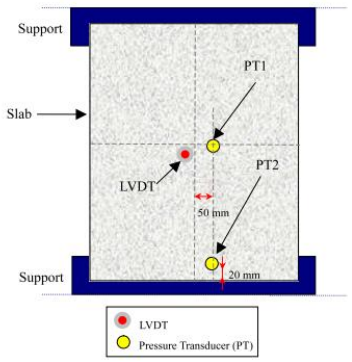

Figure 7: Points of Measuring Pressure and Impulse (Wu et al. [2])

Figure 8: Points of Measuring Pressure and Impulse (Wu et al. [2])

Table 3: Blast Wave Parameters used for Validation

Slab ID	Standoff Distance to PT1 (m)	Angle of incidence to PT2	Scaled distance, Z (m/kg1/3)	Peak reflected overpressure (kPa)	Reflected impulse (KPa.ms)	PT2/PT1
NRC-1	3	16°	3	216	147	0.88
NRC-2	3	16°	1.5	1508	668	0.86
NRC-3	1.4	32°	0.93	6153	924	0.54

The model predictions were validated herein in terms of slab deformations. The displacements response with time is shown in Figure (9.a) measured from finite element model in the center of each slab. Under the abovementioned combinations of charge weight and stand-off distance, the maximum deflections measured from finite element model in the center of each slab were 1.65, 10.92 and 13.75 mm for specimens NRC-1, NRC-2 and NRC-3, respectively. To evaluate the model, Figure (9.b) and Table (2) present the model maximum displacements at the slab center along with deviations from the results of the experimental studies. The experimental maximum displacements were predicted with maximum deviations of 10%. These results clearly show that the finite element analysis technique facilitate accurate prediction of the panel response. Further details regarding the panel testing can be found elsewhere (Wu et al. [2]).

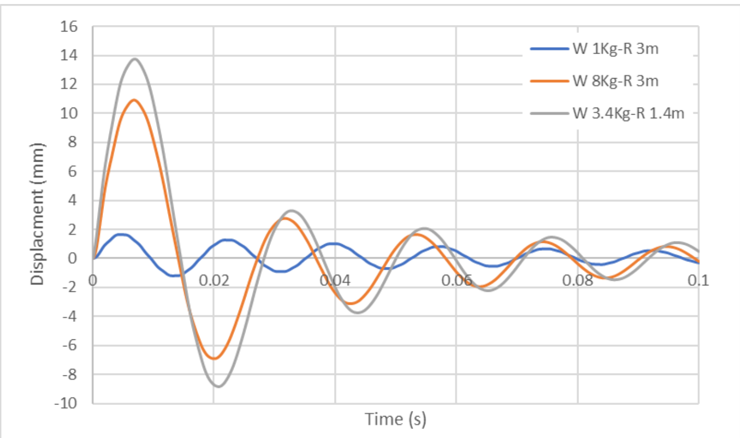

Figure 9.a: Displacements Response with Time for the Validated Slabs

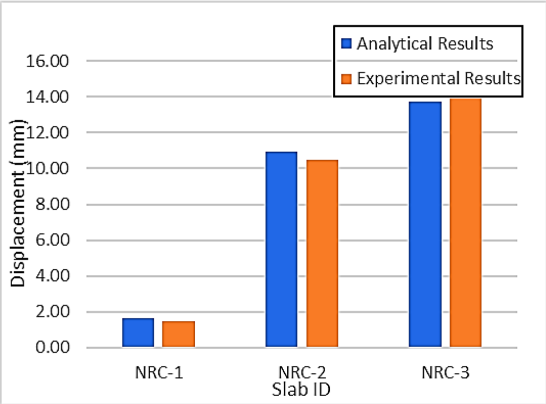

Figure 9.b: Mid-Span Deflections of Analytical Results vs. Experimental Results

Table 2: Comparison of Mid-Span Deflections with Wu et al. (2009) Experimental Results

Slab ID	Explosive Charge, W (kg)	Standoff Distance to PT1 (m)	Scaled distance, Z (m/kg1/3)	Maximum Mid-Span Deflection of Slab (mm)		Error (%)
				Wu et al. (2009) Experimental Results	Analytical Results	
NRC-1	1	3	3	1.5	1.65	10%
NRC-2	8	3	1.5	10.5	10.92	4%
NRC-3	3.4	1.4	0.93	13.9	13.75	1.1%

5- NUMERICAL STUDY

Three eight-story reinforced concrete buildings consist of different shear walls systems are considered in this parametric study. These buildings were well designed on gravity and lateral loads according to the ECP 2012 [20] by Nasr et al. [21]. They were modelled using different parameters that will be discussed in the following sections. Columns P-M-M interaction ratios and walls D/C ratios are less than coefficient of 1 to ensure that columns are safe and compatible with the ECP 2012 [20] requirements. Nasr et al. [21] applied performance base design on the three models using nonlinear static pushover-analysis as per ASCE 41-13 [17]. The studied buildings were designed under different load combinations according to ECP 2012 [20]. These combinations were applied by the following terms:

$$U = 1.40\,D + 1.60\,L \tag{3}$$

$$U = 1.12\,D + \alpha\,L \pm S \tag{4}$$

Where D is the dead load, L is the live load; S is the seismic load and superposition factor of the structure which is taken for the residential buildings.

The goal of this parametric study is to investigate the local and global behavior of three buildings of different reinforced concrete shear-wall structural configurations under blast loading. This is done by simulating the three buildings – designed by Nasr et al. [21] – under blast wave of explosive weight of 1000 Kg and standoff distance of 15m. The global response is explained through maximum story displacement, story drift and plastic behavior of the structure presented in formation of hinges for frame elements (beams and columns) as per ASCE 41-13 [17] and detect the status of the hinges as it will be explained in detail. While local response is explained by response of front face walls comparing their displacements at mid span, support rotations and compressive strains of concrete which indicate the level of damage.

5.1- Model Description

Material Model

The unconfined concrete material represents the concrete with no confinement for shear walls and slabs with cylindrical compressive strength of 30 MPa, young's modulus of 24100 MPa, density of 24 KN/m3 and max allowable compressive strain of 0.003. Confined concrete material represents the concrete for the beams and columns surrounded by ties with compressive strength calculated according to (Mander et al. [15]), based on the transverse reinforcement used to enhance the member strength and ductility. Regarding reinforcement bars, longitudinal and transverse reinforcement bars have yield strength of 420 MPa, young's modulus of 200 GPa and density of 7850 Kg/m3.

Model Geometry

The three eight-story reinforced concrete buildings have 5 bays for both X and Y directions. The floor-to-floor story height of each level is 3.2 m while the buildings are 25.6m tall with total width of 26.3m in both directions. 3D - Views for the three buildings are shown in Figures (10) while their plans shown in Figure (11). The Lateral load resisting system of the buildings consists of dual system shear walls and frames, whereas the gravity load carrying system comprises 200mm thickness concrete flat slab resting on reinforced concrete columns, marginal beams and shear walls. ***Building type (I)*** consists of shear walls and core of 200mm thickness in both X and Y directions. While ***building type (II)*** consists of 200 mm walls without core. In addition, ***building type (III)*** consists of shear walls with openings of 2.75 width and 1.80 height each (30% opening). Table (3) shows the designed sections of columns, beams and slabs for the three buildings. The nodes at the base of the building structure were restrained along all degrees of freedom representing fully fixed supports.

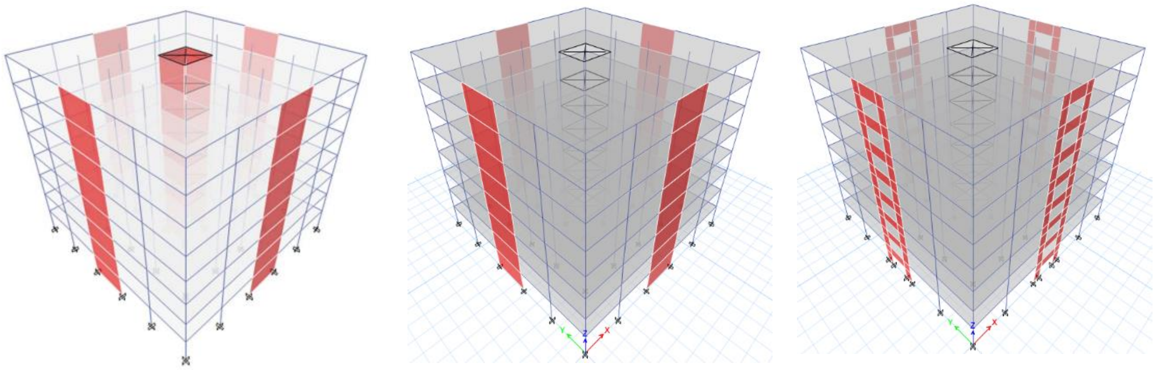

Figure 10:3D Views for *Buildings Type (I), Type (II) and Type (III)*

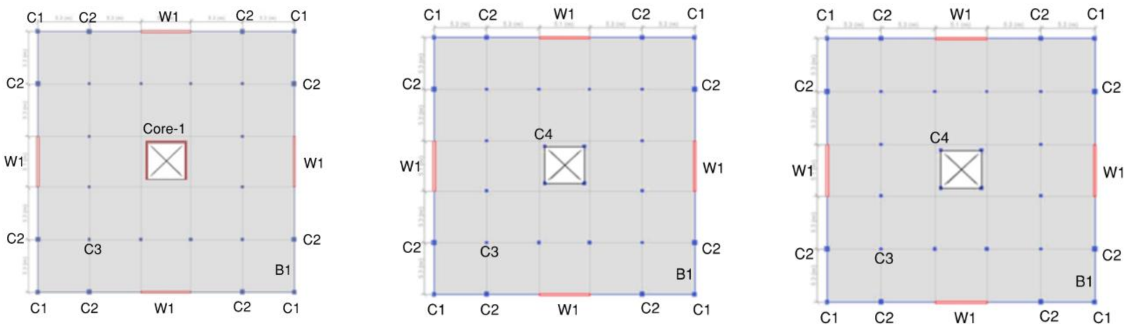

Figure 11: Plans for Buildings Type (I), Type (II) and Type (III)

Table 3: Designed Sections for the studied buildings

Columns Sections		
Column ID	**Cross-sec (mm x mm)**	**Main bars**
C1	450 x 450	16T14
C2	500 x 500	16T16
C3 (1-2)	600 x 600	20T16
C3 (3-4)	500 x 500	16T16
C3 (5-6)	400 x 400	12T14
C3 (7-8)	350 x 350	8T16
C3 (7-8)	300 x 300	8T14
C4 (1-2)	550 x 550	20T16
C4 (3-4)	500 x 500	16T16
C4 (5-6)	450 x 450	16T14
C4 (7-8)	350 x 350	8T16
Beams Sections		
Beam ID	**Cross-sec (mm x mm)**	**Reinforcement at support Upper & lower**
B1	250 x 650	11T16
Walls Sections		
Wall ID	**Thickness (mm)**	**Shear wall sections and Reinforcement VL RFT / HL RFT**
Core-1	200	T12@200 / T12@200
W-1	200	T16@200 / T12@200

Modal Analysis

The P-Delta impact on structures is taken into account in the study to account for large structural deformations. To identify the deformations, a linear analysis of the structure is performed after applying the gravity load on it initially as a static load. The rest of the analysis is carried out on the deformed condition of the structure. The structure's natural periods are determined using eigen-value analysis before the structure is analyzed for the dynamic blast loads.

Basic Models’ Loads

Gravity and seismic loads are defined in the buildings’ models by Nasr et al. [21]. The following loading assumptions have been considered for these loads:
1) Total Dead load (D) is equal to DL+SDL.
2) Dead load (DL) is equal to the self-weight of the members and slabs.
3) Super-imposed dead load (SDL) equals to 4.0 kN/m² distributed (including partitioning and 1.50 kN/m2 flooring) + wall line load 12 kN/m on perimeter beams.
4) Live Load (L) equals to 2.0 kN/m².
5) Seismic load:
- Seismic zone 3
- ground acceleration equal 0.15 ag/g
- Soil Class C

Blast Loading

As per UFC 3-340-02 [13], a surface burst is a charge that occurs on the ground surface or very close to it. The ground surface reflects and amplifies the original wave of the explosion to create a reflected wave as mentioned before. Alternative codes exist that follow metric units, as Euro Blast Report [22] and ECP – SPEC 905 [23]. For hemispherical TNT explosions, the positive phase parameters of the surface burst environment are calculated in Figure (2-15) in UFC 3-340-02 [13], while the negative phase parameters are calculated in Figure (2-15) in UFC 3-340-02 [13].

It is common knowledge that the angle of incidence is one of the factors that often influences the blast pressure on structural components. Its angle of incidence is defined as the angle formed by the outward normal and the direct vector from the explosive charge to the structural element. Blast wave used in this research with explosive weight of 1000 kg TNT at 15 m standoff distance from the longer face of the building ***(BW)*** as shown in Figure (12).

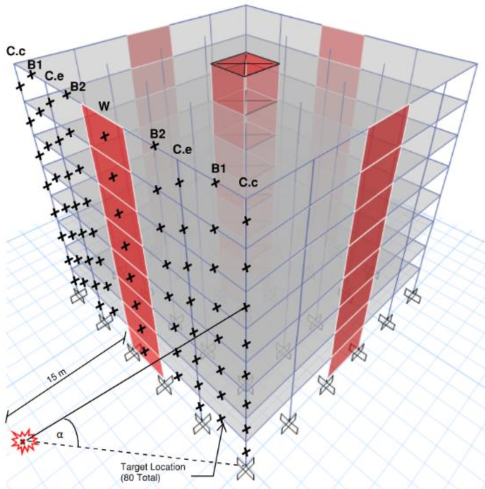

Figure 12: 3D Model Showing Blast Load Applied on Front Face

For 3D analysis, blast load is applied on each element (wall, beam and column) on front face of the building. The load time-history is determined based on the tributary area supported by the element, the actual stand-off distance between the charge location and the joint under consideration (center of structural element) as shown in Figure (12), and the angle of incidence between the wave front and the center of each element. The load on an element begins at the time when the blast wave arrives at the joint. This loading is closest to the actual loading experienced by the structure. The load on each element is calculated based on UFC 3-340-02 [13], as per the following steps:

Step 1: Determine the explosive weight of the charge, W, standoff distance from the structural element, R_G.

Step 2: Apply safety factor of 20 %.

Step 3: Determine the scaled charge distance as per Eq. (2).

Step 4: Determine the explosion's parameters using Figure (2-15) in UFC 3-340-02 [13] for the calculated scaled distance Z_G:

- Peak initial positive overpressure P_{so}
- Wave front speed U
- Scaled initial positive impulse I_s / $W^{1/3}$
- Scaled length of the positive phase t_o / $W^{1/3}$
- Scaled value of the wave arrival t_A / $W^{1/3}$
  - Multiply the scaled value with the value of W1/3 in order to obtain the absolute values.

Step 5: For the front facade:

a) Calculate the peak positive refracted pressure $P_{r\alpha} = C_{r\alpha} * P_{so}$ and read the coefficient $C_{r\alpha}$ for P_{so} (from Figure (193) in UFC 3-340-02 [13]).

b) Read the value of scaled positive refracted impulse $I_{r\alpha}$ / $W^{1/3}$ (from Figure (194) in UFC 3-340-02 [13]) for P_{so} and α.

- Multiply the scaled value with the value of W1/3 in order to obtain the absolute value.

Step 6: The duration of the equivalent triangular obliquely reflected loading shall be determined from Eq. (5):

$$t_{rf} = 2 I_{r\alpha}/P_{r\alpha} \quad (5)$$

Step 7: Calculate the tributary area for each element shown in Figure (12):

Tributary area for the beam is C.L to C.L of the story and assigned as a line load on the whole length of the beam which equals to 3.2 m2/m’ for beams of typical floors (B1 and B2) and equals to 1.6 m2/m’ for beam at roof floor (B1 and B2).

Tributary area for the walls is the exposure area to the blast load from floor to floor and assigned as an area load on the whole area of the wall.

Tributary area for the columns is the exposure area to the blast load from floor to floor and assigned as a line load on the whole length of the column which equals to 0.5 m2/m’ for edge columns (C.e) and equals to 0.45 m2/m’ for corner columns (C.c).

Step 8: Calculate the applied load on structure components:

The load applied on structure components equal to the multiplication of the peak positive refracted pressure ($P_{r\alpha}$) calculated in step 5.a and the tributary area for each element calculated in step 7.

5.2- Results and Discussion

<u>Blast Load</u>

BW parameters are determined using the previously indicated steps 1 through 8 using an explosive weight of 1000 kg TNT and a 15 m standoff distance. Based on the tributary area of each element determined as per the previously mentioned step 7, Figure (13) shows the blast load pressure time history on front walls, while Figure (14) and Figure (15) show the line load with time on front beams and columns, respectively.

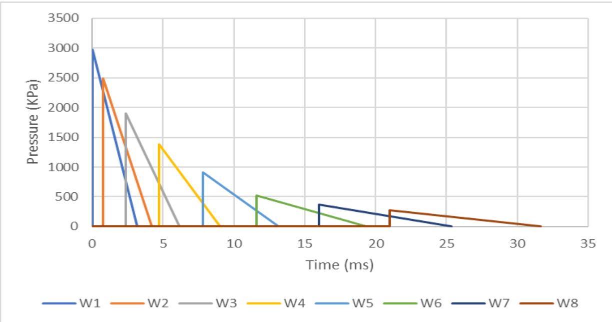

Figure 13: BW Pressure Time History on Front Walls

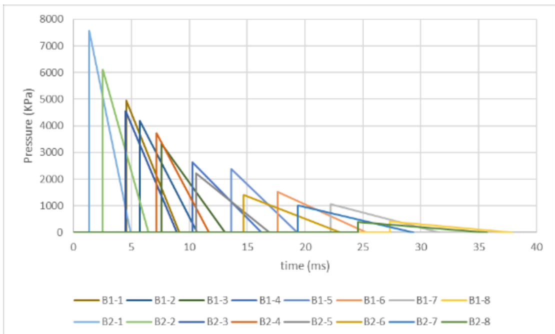

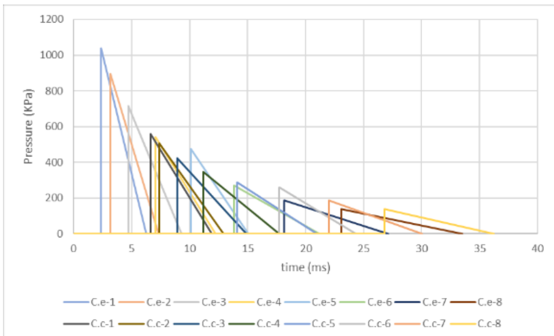

Figure 14: BW Line Load with Time on Front Beams

Figure 15: BW Line Load with Time on Front Columns

Global Response Results

➢ Status of Hinges

The first yield occurs when one hinge is formed in the stage (B to C) (the green hinge is formed). On the other hand, the ultimate point could be specified when more than one hinge is formed in the stage (>E) (hinges with red color) in one column or more. Figure (16.a) and Figure (17.a) show the formation and location of plastic hinges when the first yield occurs at 3 msec for buildings type (I) and (II), respectively. While Figure (16.b) and Figure (17.b) show the formation of plastic hinges and their locations at the end of time steps as the status of the formed hinges are (B to C) for the buildings type (I) and (II), respectively.

Regarding building type (III), Figure (18.a), Figure (18.b) and Figure (18.c) show the formation of plastic hinges from first yield stage happen to the failure stage with status (>E). Figure (18.a) shows the formation and location of plastic hinges when the first yield occurs at 3 msec. While Figure (18.b) shows the formation of the ultimate point and their locations at 250ms. In addition, Figure (18.c) shows the formation of plastic hinges and their locations as the status of hinges are (>E) at the 265ms.

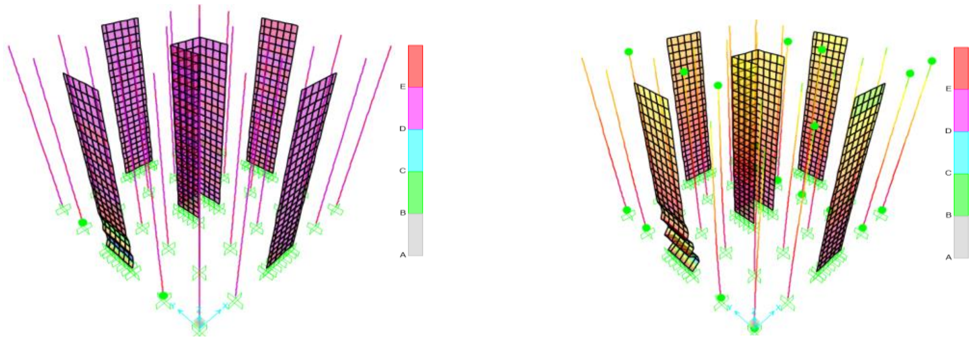

a) Hinges at First Yield **b) Hinges at the End**

Figure 16: Formation of Plastic Hinges under BW for Building Type (I)

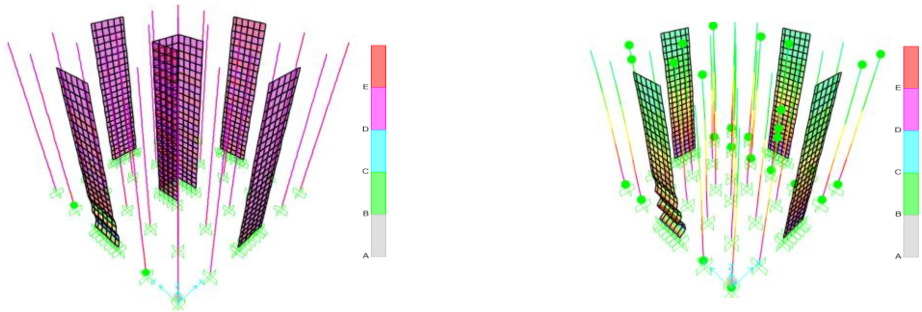

a) Hinges at First Yield **b) Hinges at the End**

Figure 17: Formation of Plastic Hinges under BW for Building Type (II)

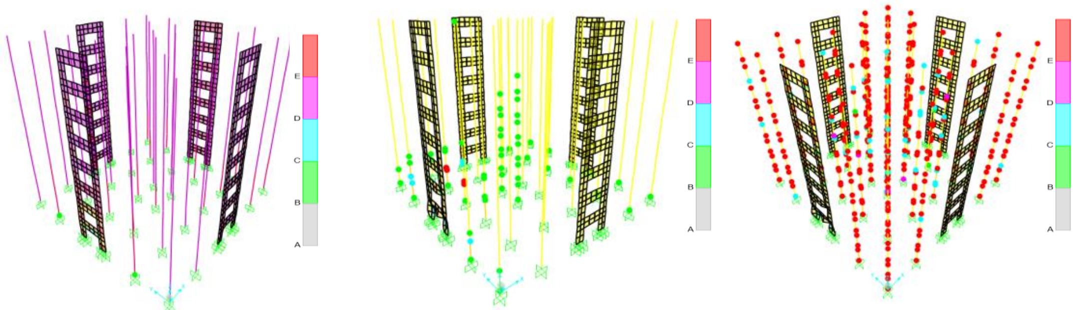

a) Hinges at First Yield **b) Hinges at Ultimate Point** **c) Hinges at the End**

Figure 18: Formation of Plastic Hinges under BW for Building Type (III)

➢ Maximum Story Displacements

Figure (19) displays maximum lateral displacement at each story level for the three studied systems. It is observed from Figure (19) that the building of type (III) totally failed as shown in the formation of the plastic hinges for the frame elements shown before, deformations at mid span and support rotations for the walls at front face as it will be explained later.

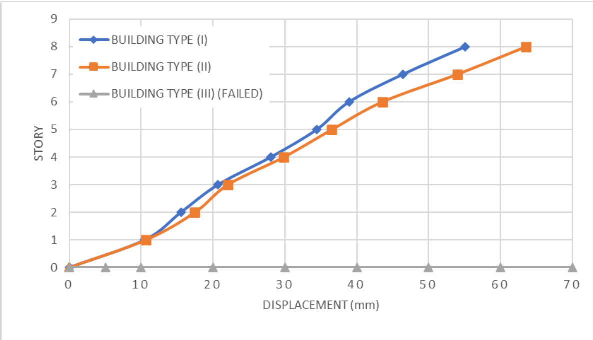

Figure 19: Maximum Story Displacements under BW

On the other hand, for type (II), the maximum story displacement increases by 15% compared to that of type (I). Figure (20) and Figure (21) illustrate the displacement – time curve for each story for the studied systems type (I) and (II), respectively. They show free vibration responses after the load has ceased to act. In all the cases analyzed here, the peak displacement of the story is achieved when the blast loads have ceased.

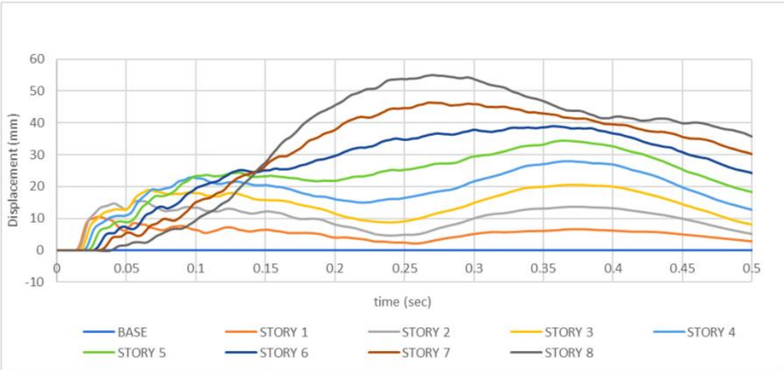

Figure 20: Story Displacement with Time under BW for Building Type (I)

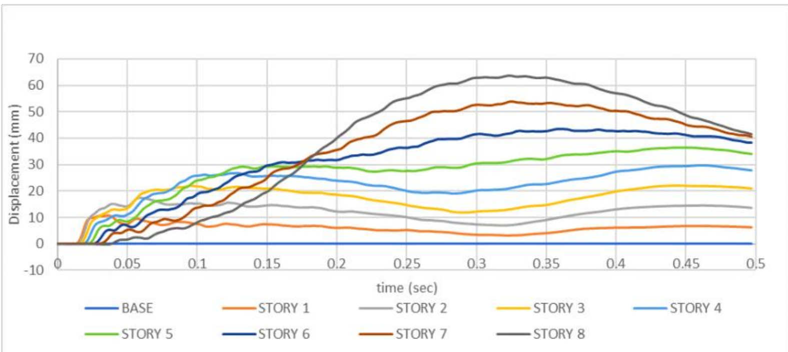

Figure 21: Story Displacement with Time under BW for Building Type (II)

➢ Maximum Story Drifts

Figure (22) shows maximum story drifts at each story level for the three studied buildings. As noted previously in story maximum displacements, building of type (III) completely failed. On the other hand, the story drift of type (II) increased by maximum of 13% compared to that of type (I).

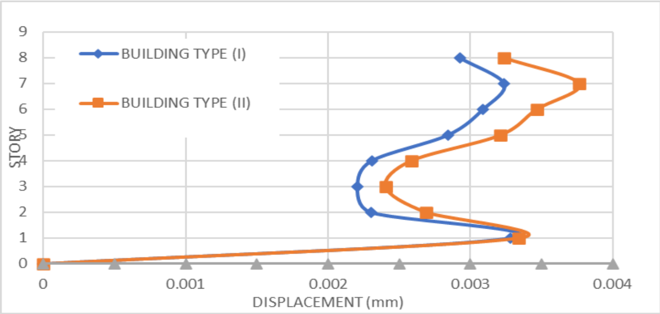

Figure 22: Maximum Story Drifts under BW

Local Response Results

➢ Walls Strains

Figure (23) and Figure (24) show the strain profile for building type (I) and (II), respectively. It is shown from these figures that the concrete crushes in compression for the first three stories as the compressive strain exceeds 0.003 for the inside and outside faces of the walls. Also, the strain of longitudinal reinforcement exceeds yield tensile strain of 0.002 for the inside and outside faces.

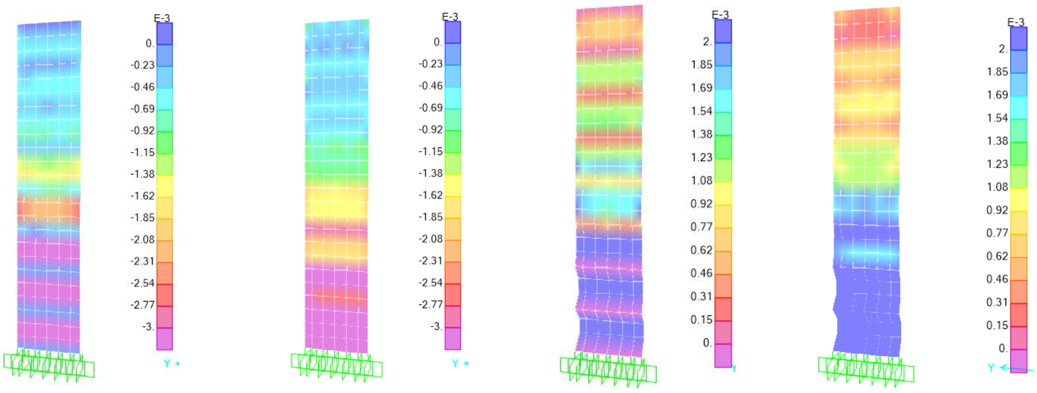

a) Compressive Strain at Inner Face **b) Compressive Strain at Outer Face** **c) Tensile Strain at Inner Face** **d) Tensile Strain at Outer Face**

Fig. 23: Strain Profile of Front Walls under BW for Building Type (I)

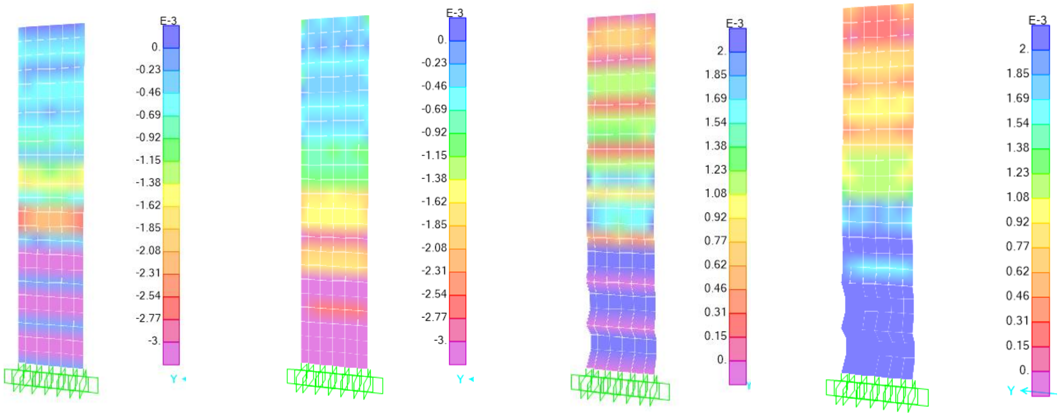

a) Compressive Strain at Inner Face **b) Compressive Strain at Outer Face** **c) Tensile Strain at Inner Face** **d) Tensile Strain at Outer Face**

Fig. 24: Strain Profile of Front Walls under BW for Building Type (II)

Regarding the strain profile for building type (III) as shown in Figure (25), all walls in the front face are completely damaged for all stories, as the concrete strain exceeds its maximum allowable strain, and longitudinal reinforcement strain exceeds its yield tensile strain for inside and outside faces.

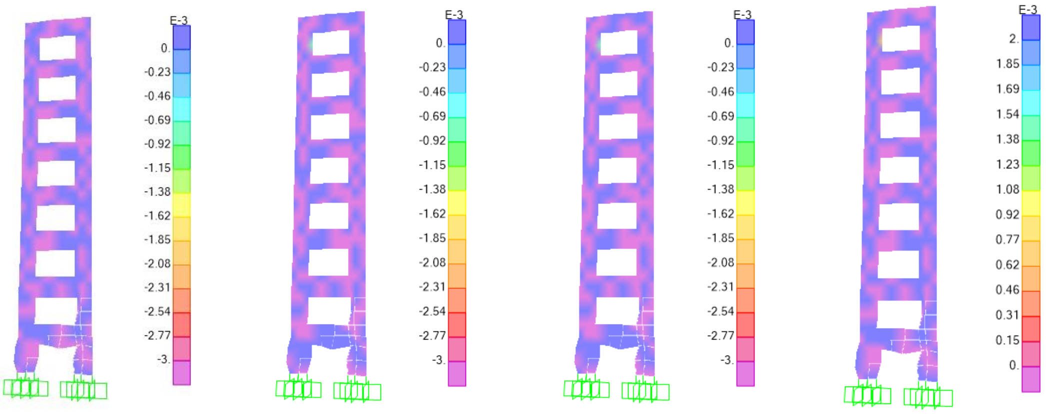

a) Compressive Strain at Inner Face **b) Compressive Strain at Outer Face** **c) Tensile Strain at Inner Face** **d) Tensile Strain at Outer Face**

Figure 25: Strain Profile of Front Walls under BW for Building Type (III)

➢ <u>Walls Displacements</u>

When duration of blast wave (td) is much shorter than the natural period of the structure (Tn). the loading is applied so quickly relative to the wall response that the wall reaches its maximum displacement after the blast load application has been completed. It can be seen that the response of curves decay after reaching the maximum displacement during the first cycle because the damping is included in the finite element model. Figure (26) and Figure (27) illustrate the out of plane displacement response at midspan of walls on the front face with time for each time step for buildings type (I) and type (II), respectively. Concerning the displacements of front face walls of building type (III), Figure (28) shows that the displacements response of the walls is increased with time during the time of observation.

It is observed that for walls at high story levels, the walls displacements at mid span increase significantly again after decaying due to the influence of global response because of the free vibration of the structure. For this reason, the local displacement at mid of walls does not reflect the real deformation as the real displacement should be calculated as the difference between displacement at midspan of the wall and that at the support (story level) at each time, as done in the support rotation calculations in the next section.

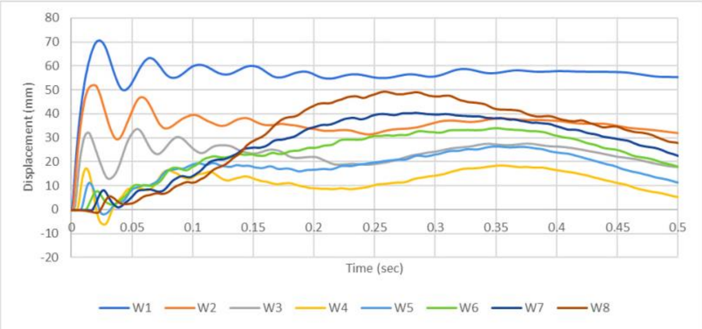

Figure 26: Displacements Response with Time at Centre of Front Walls under BW for Building Type (I)

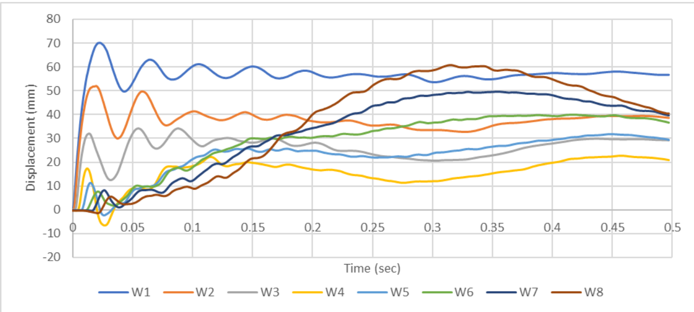

Figure 27: Displacements Response with Time at Centre of Front Walls under BW for Building Type (II)

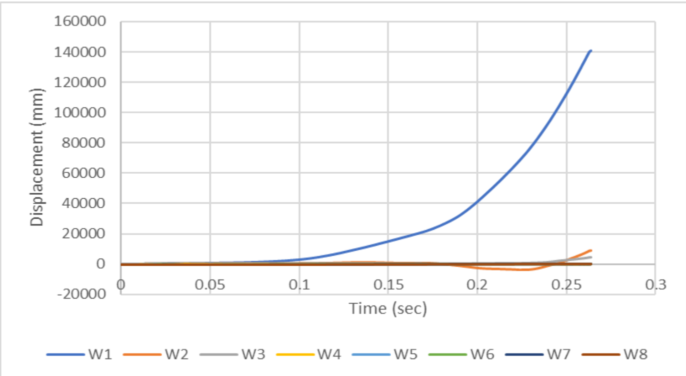

Figure 28: Displacements Response with Time at Centre of Front Walls under BW for Building Type (III)

➢ Walls Support Rotations

Regarding the support rotations, it is measured as the angle of rotation for the upper and lower supports, calculated from the maximum displacement at mid-wall relative to half the height. Under the given blast scenario, the maximum displacement can be calculated by calculating relative displacement between mid-span of the wall to the upper and lower story level for each time step through which we can get the maximum displacement as it is the maximum relative displacement through the whole-time steps.

Table (4) shows the maximum support rotations at mid-span of walls on the front face for the three systems considered. It is observed that the maximum support rotations of walls for type (I) and (II) are almost equal for the first 5 stories, while for the upper three stories for type (II) increased up to 28% compared to that of type (I). In addition, for type (III), – as shown in Table (4) – walls for the first three stories are completely damaged with excessive support rotations, while for the rest of the walls, the maximum support rotation increases up to 760% compared to that of type (I) and this percentage decreases gradually till 56% in the upper story and increased by 760% to 31% compared to that of type (II).

Table 4: Support Rotations at Centre of Front Walls under BW

Element	Building Type (I)	Building Type (II)	Building Type (III)
W1	2.527	2.530	89.486
W2	1.669	1.673	88.012
W3	0.961	0.972	83.704
W4	0.515	0.516	4.428
W5	0.339	0.340	1.335
W6	0.249	0.309	0.712
W7	0.235	0.300	0.539
W8	0.239	0.284	0.374

6- SUMMARY AND CONCLUSIONS

This study aims to investigate the global and local response of three 8-story reinforced concrete shear-wall buildings with different configurations under blast wave of explosive weight of 1000Kg TNT and 15m standoff distance. The configurations taken into consideration are the shear walls and core system, shear walls system without core and shear walls with openings system. The global response is explained by the status of plastic hinges, story displacements and maximum story drifts. In, addition, the local response is investigated by walls strains indicating the percentage of damage of the walls, the walls displacements and walls support rotations. This is done by simulating the buildings with 3D finite element modelling using SAP2000 v23, which validated by experimental results in literature (Wu et al. [2]). Based on the above discussions, the following conclusions can be derived:

1) Finite element model using SAP2000 showed to be efficient and accurate for simulating reinforced concrete panels subjected to blast loading.

2) The building of shear walls with openings completely damaged under both local and global responses under the studied blast wave.
3) The global response is enhanced by increasing the stiffness of the building, as the building of walls with openings of least stiffness completely damaged in global response results, while the building of shear walls and core got better global response in terms of lower story displacements and story drifts by around 15% than that of the building of shear walls only.
4) It is important to study both the global and local responses of buildings under blast loading, as the building of shear walls and core got lower walls support rotations for local response by around 28% than that of building with shear walls only, while it got lower story displacements indicating the global response by around 15% only.
5) For walls at high story levels, the local response results at mid span increase significantly again after decaying to reach the maximum displacement at time when the maximum story displacement occurs for the building because of the free vibration of the structure. For this reason, the local displacement at mid of walls does not reflect the real deformation to determine the level of damage and support rotation as the real displacement is the difference between displacement at midspan of the wall and that at the support (story level) at each time.

7- REFERENCES

[1] Dan Nourzadeh, J. Humarb and A. Braimahb, “Comparison of Response of Building Structures to Blast Loading and Seismic Excitations”, Procedia Engineering 210, PP: 320–325, 2017.
Available: https://doi.org/10.1016/j.proeng.2017.11.083

[2] C. Wu, D. Oehlers, M. Rebentrost, J. Leach, A. Whittaker, “Blast testing of ultra-high-performance fiber and FRP-retrofitted concrete slabs”, Engineering Structures 31 (9) (2009) 2060–2069.
Available:https://www.sciencedirect.com/science/article/abs/pii/S0141029609001151?via%3Dihub

[3] Nourzadeh, D., Humar, J.L. and Braimah, A., “Global response of building structures to blast loading: Case study of a 10-storey building”, 11th International Conference on Shock & Impact Loads on Structures, Ottawa ON, 2015.

[4] C. J. Naito, M.ASCE and K. P. Wheaton, “Blast Assessment of Load-Bearing Reinforced Concrete Shear Walls”, Pract. Period. Struct. Des. Constr. 2006.11:112-121.

[5] Osman Shallan, Atef Eraky, Tharwat Sakr, Shimaa Emad, “Response of Building Structures to Blast Effects”, International Journal of Engineering and Innovative Technology, Volume 4, Issue 2, 2014.
Available:https://www.humanitarianlibrary.org/sites/default/files/2018/10/IJEIT1412201408_30.pdf

[6] Alaa I. Chehab, A.M.ASCE, Christopher D. Eamon, M.ASCE, and Joshua Griffin, “Collapse Resistance of RC Moment-Resisting Frame and Shear Wall Structural Systems Exposed to Blast”, J. Perform. Constr. Facil., 04016099, 2016.
Available: https://ascelibrary.org/doi/10.1061/%28ASCE%29CF.1943-5509.0000957

[7] Izzuddin, B.A, Vlassis, A.G, Elghazouli, A.Y and Nethercot, D.A ―Progressive collapse of multi-storey buildings due to sudden column loss — Part I: Simplified assessment framework‖ Engineering Structures 30 (2008) 1308–1318.
Available:https://www.sciencedirect.com/science/article/abs/pii/S0141029607002805?via%3Dihub

[8] McConnell, J.R and Brown, H ―Evaluation of progressive collapse alternate load path analyses in designing for blast resistance of steel columns‖ Engineering Structures 33 (2011) 2899–2909.
Available: https://doi.org/10.1016/j.engstruct.2011.06.014

[9] Shi,Y, Li, Z.X and Hao, H ―A new method for progressive collapse analysis of RC frames under blast loading‖ Engineering Structures 32 (2010) 1691 1703.
Available:https://www.sciencedirect.com/science/article/abs/pii/S0141029610000593?via%3Dihub

[10] Hrvoje Draganić and Vladimir Sigmund, “Blast Loading on Structures”, Tehnički vjesnik 19, 3, 643-652, 2012.

[11] Ayush Meena, P.V. Ramana. “Assessment of structural wall stiffness impact due to blast load”. Materials Today: Proceedings, 2021.

Available: https://doi.org/10.1016/j.matpr.2021.03.093

[12] Krauthammer, T. (2008). Modern Protective Structures. CRC press, Boca Raton. Li, J., and Hao, H. (2011). “Development of a Simplified Numerical Method for Structural Response Analysis to Blast Load.” Procedia Engineering, Elsevier, 14, 2558–2566.
Available: https://doi.org/10.1201/9781420015423
[13] USDOD (Unified Facilities Criteria). (2008). “Structures to resist the effects of accidental explosions.” UFC 3-340-02, U.S. Dept. of Defense, Washington, DC.
[14] The 14th World Conference on Earthquake Engineering October 12-17, 2008, Beijing, China architectural and structural design for blast resistant buildings Zeynep Koccaz, Fatih Sutcu and Necdet Torunbalci.
[15] Mander, J. B., Priestley, M. J. N., and Park, R. (1988). “Theoretical Stress-Strain Model for Confined Concrete.” Journal of Structural Engineering, 114(8), 1804–1826.
[16] Z. W. Miao, X. Z. Lu, J. J. Jiang, L. P. Ye, “Nonlinear FE Model for RC Shear Walls Based on Multi-layer Shell Element and Microplane Constitutive Model”, Computational Methods in Engineering and Science, 2006.
Available: https://link.springer.com/chapter/10.1007/978-3-540-48260-4_50
[17] ASCE (2014), “Seismic evaluation and retrofit of existing buildings”, ASCE 41-13, Reston, VA.
[18] Federal Emergency Management Agency (FEMA), (1997) “Prestandard and Commentary for the Seismic Rehabilitation of Buildings” (FEMA 356), Washington, DC, October 1997.
[19] CSA (Canadian Standards Association). (2012). “Design and assessment of buildings subjected to blast loads.” CSA S850-12, Mississauga, ON, Canada.
[20] ECP (2012) ECP-201: Egyptian code for calculating loads and forces in structural work and masonry. Housing and Building National Research Center. Ministry of Housing, Utilities and Urban Planning, Cairo.
[21] Nasr E. Nasr, M. N. Fayed, Gamal Hussien, A. M. EL-Makhlasawi, “Evaluation of Seismic Response Modification Factor for Shear Wall with Openings in Multi-Story Frame Buildings”, IOSR Journal of Mechanical and Civil Engineering (IOSR-JMCE), 2021.
[22] “Calculation of Blast Loads for Application to Structural Components”, “European Laboratory for Structural Assessment”, 2013.
[23] ECP – SPEC 905, “Egyptian Specification for Blast Resistant Buildings”, 2016.